Biogeochemistry (2011) 104:5–22
DOI 10.1007/s10533-009-9352-6

Tropospheric $^{14}CO_2$ at Wellington, New Zealand: the world's longest record

Kim I. Currie · Gordon Brailsford · Sylvia Nichol · Antony Gomez · Rodger Sparks · Keith R. Lassey · Katja Riedel

Received: 17 September 2008 / Accepted: 14 July 2009 / Published online: 5 August 2009

Abstract Measurements of near-sea-level tropospheric $\Delta^{14}CO_2$ have been made at Wellington, New Zealand since December 1954; these measurements comprise the longest such record available. The $\Delta^{14}C$ rose from −10‰ in 1955 peaking at 695‰ in 1965 as a result of "bomb ^{14}C" production, before falling thereafter to the present day (2005) value of 73‰. The $\Delta^{14}C$ peak occurred about 1 year later in the southern hemisphere than in the northern hemisphere. The post-1965 fall is due to the transfer of ^{14}C-enriched CO_2 to the biospheric and oceanic pools together with ongoing release of ^{14}C-free CO_2 from fossil fuel combustion, during an era without major atmospheric nuclear-weapon tests. Time series analysis of the data using Loess decomposition and filtering indicates an approximately exponential decline in excess $\Delta^{14}CO_2$ over 1967–2005 with an e-folding time of 18 years. The seasonal cycle from 1954 until 1980 had a maximum in the late (austral) summer, a minimum in winter, with peak-to-trough amplitude that peaked at 20‰ in 1966. For the period 1980–1989, a new seasonal cycle emerged, with a maximum in winter and a minimum in late summer/early autumn and peak-to-trough amplitude of 3.5‰, transitioning to a new seasonal structure after about 1990.

Keywords $^{14}CO_2$ · Radiocarbon · Carbon cycle · Bomb pulse

K. I. Currie (✉)
Department of Chemistry, University of Otago, National Institute of Water and Atmospheric Research (NIWA), P O Box 56, Dunedin, New Zealand
e-mail: k.currie@niwa.co.nz

G. Brailsford · S. Nichol · A. Gomez · K. R. Lassey · K. Riedel
National Institute of Water and Atmospheric Research (NIWA), Wellington, New Zealand

R. Sparks
Rafter Radiocarbon Laboratory, GNS Science, Lower Hutt, New Zealand

Introduction

Natural $^{14}CO_2$ is produced in the upper atmosphere by the capture of cosmic flux derived neutrons on atmospheric ^{14}N. The resulting "cosmogenic" ^{14}C is rapidly oxidized to ^{14}CO and then to $^{14}CO_2$ which is then distributed throughout global carbon reservoirs, in particular the atmosphere, oceans and terrestrial biosphere. Prior to the Industrial Revolution the radioactive decay of ^{14}C (half-life 5,730 years) approximately balanced the natural production resulting in a near steady-state ^{14}C distribution.

Measurement programmes of atmospheric $^{14}CO_2$ have been conducted at several northern and southern hemisphere sites, including remote background stations (Manning et al. 1990; Nydal and Lovseth 1983),

and locations which reflect local modification by human activities (Levin et al. 1995, 1980; Meijer et al. 1995).

The present day atmospheric $^{14}CO_2$ burden results from the effects of the natural response to human perturbations of the carbon and ^{14}C cycles. Fossil fuel burning produces carbon dioxide which, although devoid of $^{14}CO_2$, affects the $\Delta^{14}CO_2$ through dilution, viz. the Suess effect (Suess 1955). Data from tree rings indicate that the Suess effect was causing a measurable decrease in atmospheric $\Delta^{14}CO_2$ starting from about 1890 (Stuiver and Quay 1981). Nuclear power facilities produce minor amounts of $^{14}CO_2$ that are not yet globally influential (Hesshaimer et al. 1994), though are considered by Naegler and Levin (2006). The detonation of nuclear weapons during atmospheric testing in the 1950s and 1960s produced large neutron fluxes which reacted with atmospheric ^{14}N to produce ^{14}C by the same process as cosmogenic ^{14}C production. While the majority of the atmospheric bomb tests ceased after the Test Ban Treaty of 1963, non-signatories France and China continued atmospheric testing until 1968 and 1980, respectively (Nydal and Gislefoss 1996). This so-called "bomb ^{14}C" increased the global atmospheric burden of ^{14}C by approximately 70% in the mid-1960s. The global mean peak atmospheric $\Delta^{14}CO_2$ occurred in 1965 (Hua and Barbetti 2004); in the northern hemisphere the $\Delta^{14}CO_2$ peak occurred earlier and was of greater magnitude than the southern hemisphere peak (Manning et al. 1990; Nydal and Lovseth 1983).

Since the mid-1960s the atmospheric $^{14}CO_2$ burden has fallen due to its transfer to other carbon reservoirs. Enhanced levels of $^{14}CO_2$ are now evident in many other carbon pools, including the oceans (e.g. Broecker et al. 1980, 1985), tree rings (e.g. Cain and Suess 1976; Hua and Barbetti 2004; Stuiver and Quay 1981), soil horizons (e.g. Milton and Kramer 1998; O'Brien 1986), corals (e.g. Druffel and Suess 1983) and ice cores (e.g. Levchenko et al. 1997). The distribution of the bomb carbon spike has proved a useful tracer for determining dynamics among the carbon reservoirs, and for teasing out the various underlying processes. A test of global models of CO_2 cycling in the oceans and biosphere is that they are able to account for the atmospheric $^{14}CO_2$ record.

Differences in $\Delta^{14}CO_2$ between the southern and northern hemispheres occur due to the relative importance of different sources and sinks in the two hemispheres, and the slow inter-hemispheric mixing times. More fossil fuel burning occurs in the northern hemisphere due to greater land area and higher population thereby causing a regional Suess effect (Levin et al. 1995). The terrestrial biosphere influence is also greater in the northern hemisphere. In contrast, the southern hemisphere is dominated by oceanic exchange and exhibits lower $^{14}CO_2$ latitudinal gradients and smaller seasonal variation. A minimum in atmospheric $\Delta^{14}CO_2$ has been identified at mid-high southern latitudes due to exchange with the Southern Ocean (Levin and Hesshaimer 2000). El Niño-Southern Oscillation (ENSO) events may also result in variations in atmospheric $^{14}CO_2$ due to changes in the upwelling rate of deep ^{14}C-depleted water in the equatorial Pacific Ocean (Rozanski et al. 1995).

Using a global carbon cycle model and the IPCC "business-as-usual" scenario, Caldeira et al. (1998) predicted that the atmospheric $^{14}CO_2$ burden will continue to decline until early in the 21st century, and increase thereafter as natural $^{14}CO_2$ production, diluted by fossil-derived CO_2, is overtaken by the increasing net ocean/biosphere return of $^{14}CO_2$ to the atmosphere. However, atmospheric $\Delta^{14}CO_2$ will continue to decline.

The oceans are predicted (Caldeira et al. 1998) to become a net source of tropospheric ^{14}C in the middle of the current century as the $^{14}CO_2$ concentration in the ocean increases due to changing isotopic partitioning of the oceanic inorganic carbonate species, and the partial pressure of $^{14}CO_2$ in the ocean becomes greater than that in the overlying atmosphere. The prediction of the timing of these events is sensitive to the accuracy of the calculated bomb carbon production rate, and to details of the parameterisations of the biospheric and oceanic fluxes (Naegler and Levin 2006).

Measurements of tropospheric $^{14}CO_2$ have been made at Wellington, New Zealand (Fig. 1), since December 1954, which was just before the major injection of bomb-produced ^{14}C in the northern hemisphere. These measurements comprise the longest such record in the world and have previously been reported by Rafter and Fergusson (1957), Manning et al. (1990), and Manning and Melhuish (1994). The data have recently contributed to the construction of a global ^{14}C data set for use in

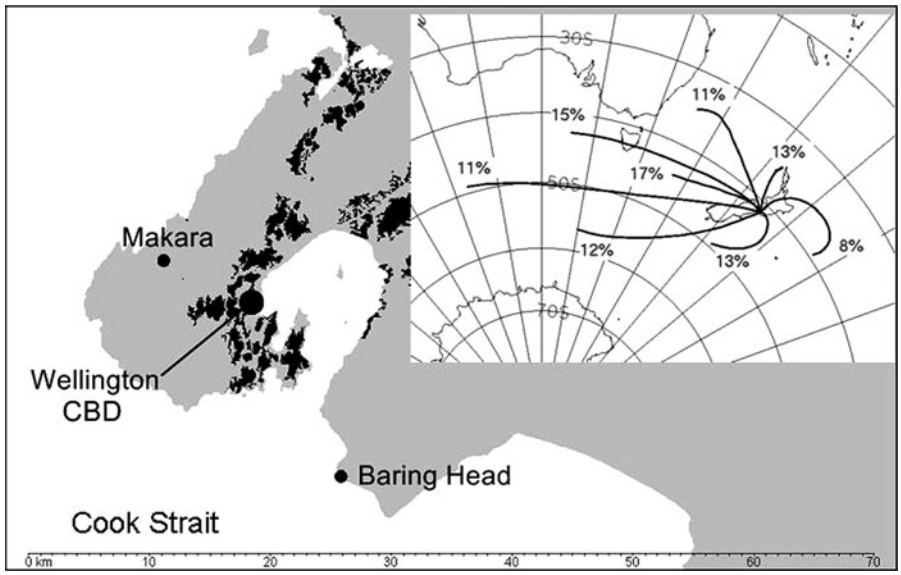

Fig. 1 Map of the lower North Island of New Zealand, showing the locations of the sampling sites at Makara (41.25°S, 174 69°E) and Baring Head (41.41°S, 174.87°E), 23 km apart. A map of New Zealand is shown in the *inset* with trajectory clusters for a period 1990–1999 indicating the origin of air masses arriving in Wellington. Mean trajectories and their proportional occurrences are shown for eight clusters (identified using cluster analysis) of Wellington 4-day back trajectories for the period 1990–1999

modeling and in calibration of carbon dating calculations (Hua and Barbetti 2004).

This paper updates the Wellington time series to 2005 and analyses the dataset for long-term and seasonal trends, and inter-annual variability. The Wellington data are compared with data from another southern hemisphere site at a similar latitude, Cape Grim, Australia (40.68°S, 144.68°E).

Methods

An atmospheric $^{14}CO_2$ measurement programme was initiated in Wellington, New Zealand in 1954 (Rafter 1955; Rafter and Fergusson 1957). For the first 33 years, samples were collected from Makara (41.25°S, 174.69°E, 300 m asl), on the west coast of the North Island (see Fig. 1). In 1987 the collection site was moved to the Baring Head atmospheric sampling station (41.41°S, 174.87°E, 80 m asl; Fig. 1), situated on the south coast of the North Island, 23 km from the original Makara site. The sampling and analytical methods used in the programme have changed only slightly over the years, as described below.

The samples have all been collected by static absorption of atmospheric CO_2 into a solution of carbonate–free NaOH (5 mol l^{-1}). From 1954, a Pyrex® tray of NaOH was exposed to the atmosphere for intervals of 1–2 weeks. In 1999 the collection method changed to using a high density polyethylene (HDPE) bottle containing the same concentration of NaOH solution as the tray, and exposed to the overlying atmosphere within a Stevenson meteorological screen by removing the lid. This change, which was implemented due to safety issues surrounding the handling of large trays of highly caustic solution, was made possible by a change in the analytical method in 1995 which reduced the sample-size requirement by a factor of 1,000. The two collection methods (tray and exposed bottle) have been compared by simultaneously using both methods, on two separate occasions. This comparison indicates that there is no significant difference between the two methods (Table 1).

The CO_2 was extracted from the exposed NaOH solution by acidification followed by cryogenic distillation (Rafter and Fergusson 1959). The ^{14}C in the extracted carbon dioxide was determined by gas proportional counting until May 1995 and then by accelerator mass spectrometry (AMS). All ^{14}C measurements were carried out at the Rafter Radiocarbon Laboratory, GNS Science (formerly Institute of Nuclear Sciences, DSIR), New Zealand. The isotope fractionation which occurs during CO_2 absorption has been corrected for using the measured $\delta^{13}CO_2$ of the extracted gas. The reported $\Delta^{14}CO_2$ values are normalized to a $\delta^{13}C = -25‰$ and are the deviations of the measured ^{14}C content relative to the ^{14}C

Table 1 Comparison of the exposed tray and exposed bottle methods for absorption of atmospheric carbon dioxide

	Exposed tray #1	Exposed bottle #1	Exposed tray #2	Exposed bottle #2
Volume of NaOH/ml	2000	125	2000	125
Mid-date of exposure	29 March 2005	29 March 2005	16 April 2005	16 April 2005
Duration of exposure/days	16	16	20	20
$\delta^{13}C$/‰	−19.90	−18.04	−18.35	−19.06
$\Delta^{14}C$/‰ (AMS error)	71.4 (2.3)	74.5 (2.3)	80.5 (2.1)	77.4 (2.0)

Modern Standard (Donahue et al. 1990; Stuiver and Polach 1977):

$$\Delta^{14}C_{sample} = \frac{A_S}{A_{abs}}\left(\frac{0.975}{1+\delta^{13}C_{sample}}\right)^2 - 1 \quad (1)$$

where A_S and A_{abs} are the $^{14}C/C$ molar ratios in sample and standard, respectively, with an accepted value for A_{abs} of 1.176×10^{-12} (Karlen et al. 1964; Stuiver and Polach 1977), equivalent to 50.6×10^9 atom(^{14}C) g $(C)^{-1}$. While the usual "per mil" notation, ‰, is used to express both $\delta^{13}C$ and ^{14}C numerically, the implied scaling factor of 1,000 is omitted from algebraic expressions such as Eq. (1).

Since the static exposure method absorbs carbon dioxide over a 1–2 week period each sample will represent many different air masses, so that the origin of those air masses can be important. Due to New Zealand's location in the mid-latitude zone of predominately westerly airflow, the broad scale airflow to Wellington is mainly from the west (Fig. 1). About 40% of the time the airflow is from the west, 25% of the time it is from the north, and about 25% of the time it is from the south-west or south (unpublished data). Airflow from the north and west is influenced by terrestrial sources, including rural land and, on occasions, Wellington city. Airflow from the south and south-west to Baring Head is influenced by the ocean (Gomez 1996), whereas at Makara it can be influenced by terrestrial sources. The tropospheric CO_2 mixing ratio measured at Baring Head during northerly conditions is, on average, within ±5 ppm of that measured during southerly conditions, therefore any anthropogenic effect on the measured $\Delta^{14}CO_2$ is likely to be minor.

Results

The time series measurements reported here constitute the longest record of ^{14}C in atmospheric carbon dioxide in the world. The $\Delta^{14}CO_2$ data are in Table 3 in the Appendix and displayed in Fig. 2. The data are

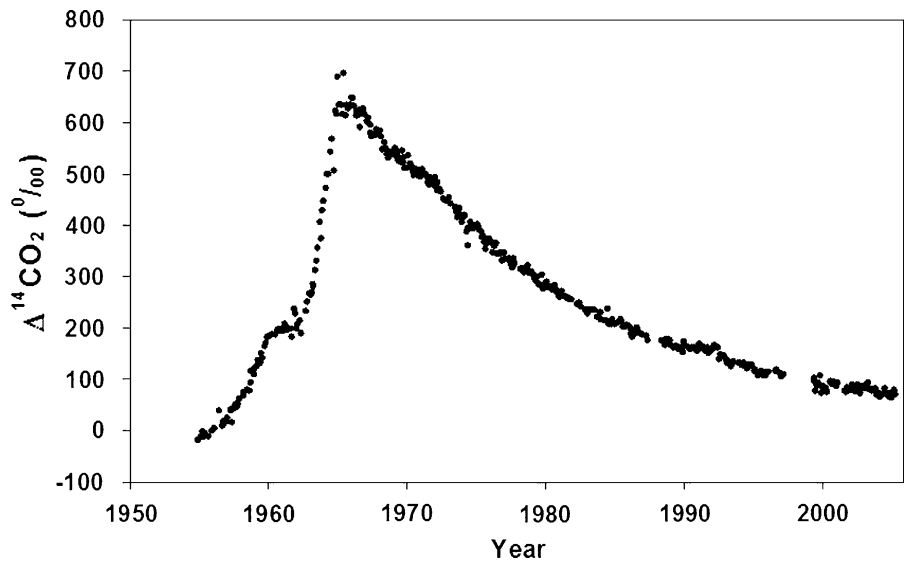

Fig. 2 The time series of atmospheric $\Delta^{14}CO_2$ measured at Wellington, New Zealand from 1954 to 2005. The data are in Table 3 in the Appendix

also available from http://gaw.kishou.go.jp/wdcgg/. Some of the values have been revised since being presented by Manning et al. (1990), as indicated in the Appendix.

At Wellington, $\Delta^{14}CO_2$ increased from −10‰ in 1955, to a peak of 695‰ in 1965 as a result of bomb ^{14}C generation. This observed peak was smaller and occurred 1 year later than in the northern hemisphere (Levin et al. 1985; Nydal and Lovseth 1983). After 1965 $\Delta^{14}CO_2$ decreased in response to the combination of the near-complete cessation of atmospheric nuclear bomb tests, oceanic and terrestrial CO_2 uptake, and dilution by fossil CO_2. The present day (2005) $\Delta^{14}CO_2$ value is 73‰. The e-folding time has been relatively constant at ca 18 years for the post-bomb decrease (1967–2005) in excess $\Delta^{14}CO_2$.

Seasonal variability in $\Delta^{14}CO_2$ at Wellington

A Seasonal-Trend decomposition procedure based on Loess (STL) filtering (Cleveland et al. 1983) has been used to analyse the Wellington $\Delta^{14}CO_2$ data set (Fig. 3). The STL procedure involves decomposing the time series into trend, seasonal and residual components (Cleveland et al. 1983). The STL procedure was used by Manning et al. (1990) to analyse the Wellington $\Delta^{14}CO_2$ dataset (with data from 1954 to 1987).

Manning et al. (1990) reported that up until 1980 the seasonal component for the Wellington time series had a maximum in March, and a minimum in August. Manning et al.'s (1990) STL analysis of the data for the period 1965–1987 showed the amplitude of the seasonal component decreasing steadily from a peak-to-trough range of 20‰ in 1966 to 3‰ in 1980. From 1980 to 1987, Manning et al. (1990) report the emergence of a new cycle with amplitude of 5‰, a maximum in July–August and a minimum in January. They concluded that the phase reversal was not due to stratospheric–tropospheric exchange, but was most probably due to ocean or land influences.

Our STL analysis of the updated Wellington $\Delta^{14}CO_2$ dataset, 1954–2005, confirms the seasonal cycle for the period 1966–1977 identified by Manning et al. (1990). STL analysis of the period 1967–1979 (note slightly different time period than that discussed by Manning et al. (1990)) gives a maximum in February (late austral summer), a minimum in July/August (austral winter) and a declining peak-to-trough amplitude that averages 9‰ (Fig. 4) In this study we also find that from 1980 onwards the seasonal cycle changes, and that it gets more complex. For the period 1980–1989, the maximum occurs in July, the minimum occurs in March and the mean amplitude is 4‰. While these results differ slightly from those for the period 1980–1987 reported by Manning et al. (1990) some of the data from this period have since been revised. For the period 1990–2005, the STL analysis indicates that the seasonal cycle is barely discernable (Fig. 4c).

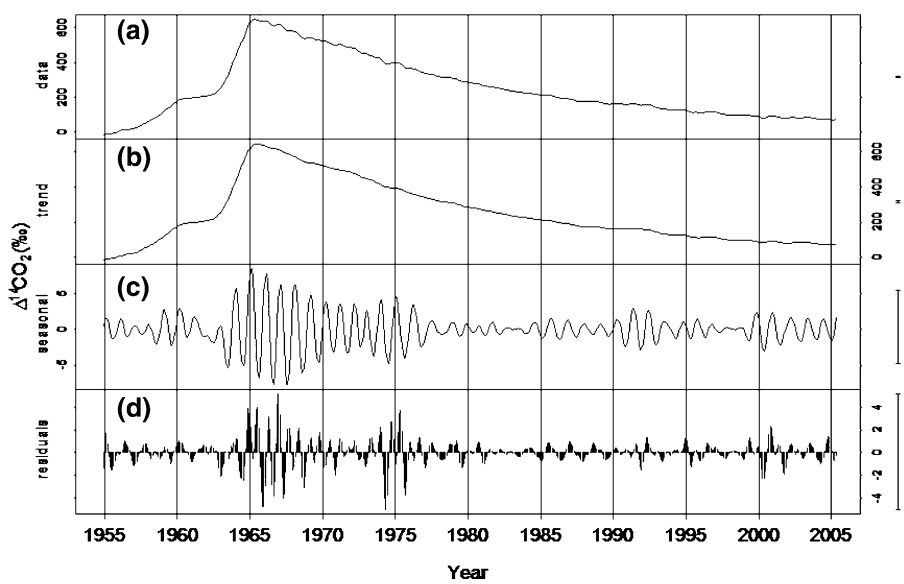

Fig. 3 The **a** smoothed data, **b** trend component, **c** seasonal component and **d** residual component of the Wellington $\Delta^{14}CO_2$ data record for 1954–2005. Analyses use the STL procedure (Seasonal-Trend decomposition based on Loess) of Cleveland et al. (1979)

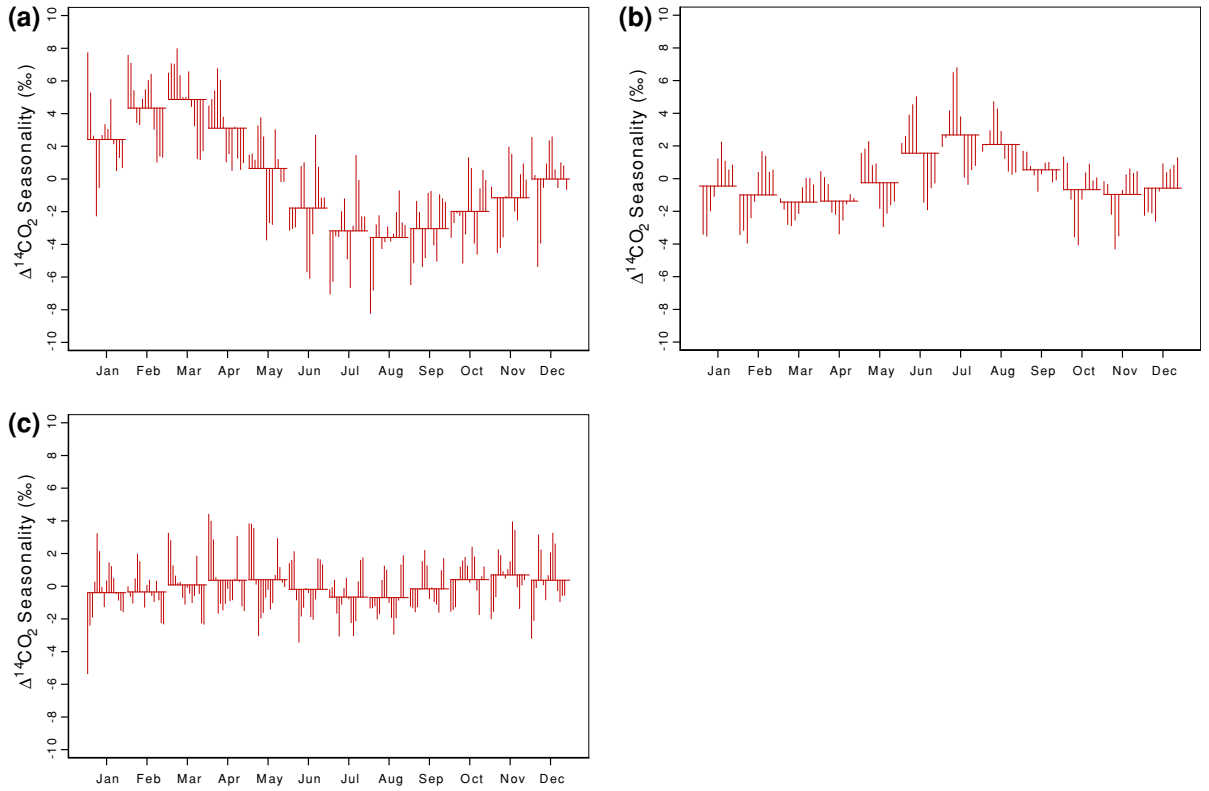

Fig. 4 Seasonal cycles of differences between $\Delta^{14}CO_2$ data and the seasonal component of the STL fitting. Data are shown as deviations from the mean in each month for the periods **a** 1967–1979, **b** 1980–1989 and **c** 1990–2005

Tropospheric inventory of $^{14}CO_2$

$\Delta^{14}CO_2$ is a measure of the $^{14}C/C$ molar ratio and therefore responds to changes in both ^{14}C and total carbon. It is useful to look at the change in the ^{14}C inventory alone, thus enabling the dynamics of ^{14}C excess (bomb ^{14}C) to be traced. The change in ^{14}C inventory can also more easily be compared with model outputs. The mixing ratio of $^{14}CO_2$ is one such measure of atmospheric ^{14}C inventory.

The tropospheric mixing ratio of $^{14}CO_2$ at Wellington can be constructed from the $\Delta^{14}CO_2$ measured at Wellington, the $\delta^{13}CO_2$ record at Cape Grim, Tasmania (Allison and Francey 2007; Francey et al. 1999) as a proxy for Wellington, and the mixing ratio of atmospheric CO_2 (XCO_2), which has been measured at Wellington from November 1970 to the present (Gomez 1996). For the period from 1958 to 1970, XCO_2 values were estimated using Mauna Loa measurements (Keeling and Whorf 2005).

We have constructed a Wellington time series for $^{14}CO_2$ mixing ratio, denoted [$^{14}CO_2$], and expressed in amol mol^{-1} (attomol $^{14}CO_2$ per mol of dry air, parts per 10^{18}), through inverting Eq. (1). This mixing ratio, presented in Fig. 5, is believed to be broadly representative of the extra-tropical southern hemisphere troposphere, and so is proportional to the $^{14}CO_2$ burden in that region of the atmosphere. From the mid-1960s when $\Delta^{14}CO_2$ gradients were weak or indiscernible, the aseasonal trend in [$^{14}CO_2$] is near proportional to that in the global atmospheric burden of $^{14}CO_2$. The peak in [$^{14}CO_2$] occurred in 1965, after which [$^{14}CO_2$] decreased until 2000 and has slowly increased thereafter. The data therefore are consistent with predictions by Caldeira et al. (1998) of a $^{14}CO_2$ inventory minimum early in the 21st century.

Discussion

Atmospheric $^{14}CO_2$ content and $\Delta^{14}CO_2$ are strongly influenced by five factors: atmospheric mixing, ocean–atmosphere exchange, terrestrial biosphere

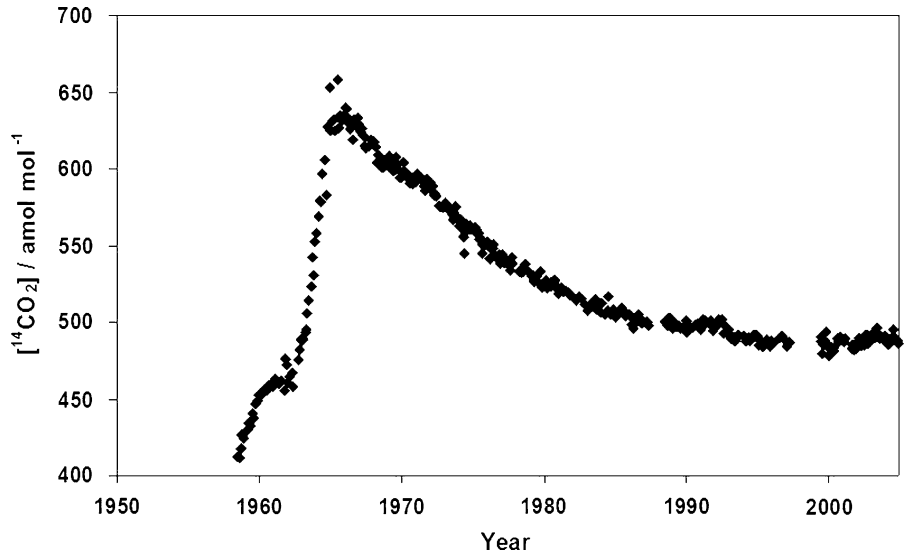

Fig. 5 The tropospheric mixing ratio of $^{14}CO_2$ at Wellington, [$^{14}CO_2$], from 1958 to 2005 (1 amol mol^{-1} = 1 part in 10^{18})

exchange and anthropogenic effects. These influences vary both temporally and spatially.

Temporal variability in $\Delta^{14}CO_2$ at Wellington

Randerson et al. (2002) used the GISS atmospheric tracer model coupled with outputs from an ocean model and a biosphere–atmosphere model to examine latitudinal and seasonal variability in tropospheric $^{14}CO_2$. By distributing the bomb $^{14}CO_2$ input according to the detonation location and by assuming no cross–equatorial mixing in the stratosphere, Randerson et al. (2002) were able to reproduce both the amplitude and the seasonality of the pre-1980 $\Delta^{14}CO_2$ seasonal cycle at Wellington. Although they were not able to reproduce the post-1980 seasonal cycle reported by Manning et al. (1990) and in this study, Randerson et al. (2002) noted that the emergence of a second seasonal cycle was consistent with the decline in the importance of the Northern Hemispheric stratospheric input to the southern hemisphere troposphere, together with the increasing relative importance of seasonal contributions from the southern hemisphere oceans and southern hemisphere stratosphere.

Randerson et al. (2002) separated the temporal variability in modeled $\Delta^{14}CO_2$ into the various inflows due to exchanges with the other reservoirs. They considered in detail the model results for the grid cell that contained New Zealand, which they then compared with the actual measurements reported by Manning et al. (1990) for Wellington. At New Zealand the amplitude (peak-to-trough) of the modeled oceanic seasonal $\Delta^{14}CO_2$ fell from 4‰ in the late 1960s to less than 1‰ in 1989. The stratospheric contribution to the modeled $\Delta^{14}CO_2$ decreased as the bomb radiocarbon was redistributed throughout the other reservoirs. For New Zealand the southern hemisphere stratospheric component of the modeled $\Delta^{14}CO_2$ seasonal amplitude fell from 2.5‰ in the late 1960s to 1‰ in 1989. The influence of the terrestrial biosphere was sensitive to the rate of carbon cycling prescribed in the model, and both the phase of the seasonal cycle and the latitudinal distribution changed during the period 1965–2000. The amplitude of the modeled influence of the terrestrial biosphere exchange on New Zealand $\Delta^{14}CO_2$ varied from 5‰ in the late 1960s to 1‰ in 1990. The fossil C contribution to the atmospheric $\Delta^{14}CO_2$ amplitude did not change significantly from 1965 to 1990, and the fossil fuel amplitude for the New Zealand region was less than 1‰ with a maximum in March (austral autumn) and a minimum in September (austral spring). These separate origins and their combined impact are summarised in Table 2.

The modeled seasonal cycle (Randerson et al. 2002) was similar to the Wellington observations (but with a time lag of 1.5 months) for the period 1960s to mid 1970s; during this period the northern

Table 2 Summary of contributing factors and their modeled and observed effects on the $\Delta^{14}CO_2$ seasonal signal at Wellington, New Zealand

Origin	Amplitude (‰)	Max	Min
Fossil fuel	1	March	Sept
Ocean exchange	4 (1960s)	Sept	March
	1 (1990s)		
Stratosphere	30 N (1960s)	Feb	July
	0 N (1990s)	Sept	March
	2.5 S (1960s)		
	1 S (1990s)		
Biosphere	4 (1960s)	Sept	March
	1 (1990s)		
Total modeled	20 (1967–1971)	Jan	July
Observed	10 (1960s)	March	August
	4 (1980s)	July	
	3 (1990s)		

Modeled values are from Randerson et al. (2002). Amplitude refers to the peak-to-trough range

hemisphere stratospheric input dominated the tropospheric signal. By the late 1980s this northern hemispheric stratospheric influence had weakened, and the southern hemispheric oceans were predicted to be the major influence on seasonality of southern hemisphere tropospheric $^{14}CO_2$.

Tropospheric inventory changes

The changes in $[^{14}CO_2]$, a proxy for the $^{14}CO_2$ burden in the local troposphere, can be interpreted using an STL analysis of the seasonal variability in $[^{14}CO_2]$ (not shown) and with reference to the GRACE model results of Naegler and Levin (2006).

The rate of change of $[^{14}CO_2]$ (Fig. 5) can be analysed in three main periods. From 1967 to 1979 $[^{14}CO_2]$ decreased at an average rate of 8 amol mol^{-1} y^{-1} ($R^2 = 0.98$), slowing to an average rate of 3 amol mol^{-1} y^{-1} ($R^2 = 0.87$) during 1980–1989. From 1990 to 2005, $[^{14}CO_2]$ was nearly constant at $\sim$490 amol mol^{-1}, and is expected to rise over ensuing decades. These periods also exhibit differing seasonality. A late summer maximum (February/March) and a winter minimum (August) occurred in the period 1967–1979. For the 1980–1989 period the amplitude of the seasonal cycle decreased, and the maximum occurred in winter (July). The maximum in the seasonal cycle for the period 1990–2005 occurred in spring (October).

The secular decline in $[^{14}CO_2]$ since 1966 can be compared with simulations in tropospheric inventory from the Global Radiocarbon Exploration (GRACE) model, as described by Naegler and Levin (2006). The GRACE model simulates global excess radiocarbon inventories for the period 1945–2005, which are in good agreement with stratospheric and tropospheric radiocarbon observations and estimates of ocean excess radiocarbon inventories from the GEOSECS and WOCE surveys (Naegler and Levin 2006). Naegler and Levin (2006) show that from 1966 to the late 1970s, the tropospheric decline was due to uptake by the oceans and biosphere exceeding the bomb ^{14}C exodus from the stratosphere. The amplitude of the $[^{14}CO_2]$ seasonal cycle was at a maximum in 1966 as the bomb carbon, mainly from the northern hemisphere stratosphere, mixed to the northern troposphere with maximum mass transport in the late boreal spring (Appenzeller et al. 1996), then into the southern hemisphere troposphere with maximum interhemispheric transport during austral spring (Hartley and Black 1995). This contribution was the major influence on the amplitude and timing of the $^{14}CO_2$ seasonal cycle from 1966 until 1979 giving a maximum in February and a minimum in August.

In the late 1970s the net biospheric and oceanic uptakes slowed, as the return $^{14}CO_2$ fluxes assumed more importance (Naegler and Levin 2006). From the late 1970s onwards, the biosphere became a net source of tropospheric $^{14}CO_2$ due to respiration and decaying vegetation returning CO_2 that was fixed when $^{14}CO_2$ was higher, and in the late 1990s the ocean is almost in ^{14}C equilibrium with the atmosphere (Naegler and Levin 2006). Interannual variability, which had previously been obscured by the bomb carbon signal became apparent, with effects from ENSO, the Southern Annular Mode (SAM) and changing sunspot activity being possible explanations of the observed variability.

Spatial variability in $\Delta^{14}CO_2$ in the southern hemisphere

Measurements of tropospheric $\Delta^{14}CO_2$ have been made in samples from Cape Grim, Tasmania, Australia (40.68°S, 144.68°E) since 1987 (Levin et al. 2007). Cape Grim is at a similar latitude to Wellington,

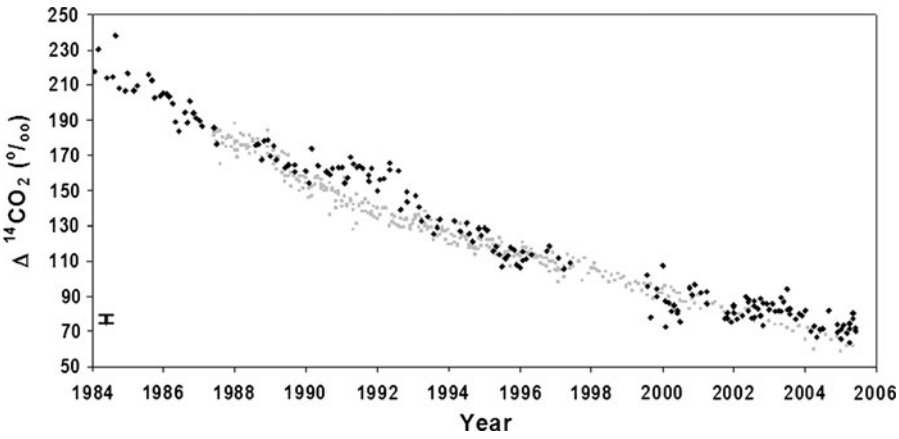

Fig. 6 Atmospheric $\Delta^{14}CO_2$ record at Wellington, New Zealand (◆) and Cape Grim, Tasmania (■) for 1987–2005. The uncertainties in the Wellington data are given in the Appendix, the average standard deviation for this time period, 3.9 ‰, is indicated by the *bar* on the *lower left hand side* of the plot

therefore allowing assessment of the longitudinal variability in $^{14}CO_2$ (Fig. 6).

The two data sets show similar gross features without an apparent longitudinal gradient. The long term trend is similar at the two sites, with an e-folding time of 18 years. More small-scale temporal structure is apparent in the Wellington record, with prominent positive departures relative to the Cape Grim record occurring in 1990–1992 and 2002–2003.

Detailed and careful examination of the Wellington data history has confirmed the reliability of the both the sampling method and the sample analysis for these two time periods, leaving us with no compelling reason to doubt their validity. The departure in 1990–1992 occurred within the duration of sampling by passive absorption into a tray of NaOH, with subsequent analysis of the extracted CO_2 by gas proportional counting. The departure in 2002–2003 occurred within the duration of sampling by absorption in a bottle of NaOH, with AMS analysis of the ^{14}C. The continuity of sampling protocol before, throughout and after each period of departure makes any undetected sampling artifact implausible. If for either period the ^{14}C determinations had incurred a systematic bias, then other ^{14}C determinations unrelated to $^{14}CO_2$ in that laboratory would have been similarly biased, yet no evidence of such a bias has been seen. Examination of the radiocarbon laboratory records for the atmospheric samples reveals that those collected between November 1988 and April 1991, i.e. from well before the onset of the departure to the middle of the departure, were measured in arbitrary order between November 1990 and May 1991. It is only when the data are ordered by date of collection that the anomalous structure is revealed. Furthermore, we have examined back-trajectories representative of the air sampled at Baring Head during 1990–1992, and have detected no systematic differences from those of subsequent years suggesting that local CO_2 sources are unlikely to have been unusually influential during 1990–1992. The source of the differences between the $\Delta^{14}CO_2$ record at Baring Head and Cape Grim is therefore not readily explained. A possible contributory cause may be unequal influences at those sites by broad-scale regional carbon cycle perturbations, possibly suggesting a transitory role by the South Pacific Ocean surrounding New Zealand.

The Randerson et al. (2002) model identified changes to the spatial distribution of $\Delta^{14}CO_2$ that have changed over the last few decades, in particular the weakening of the north-south gradient profile and the northern hemisphere fossil fuel signal being offset by the terrestrial impact. Many ecosystems are becoming sources of atmospheric $^{14}CO_2$ as the biospheric production of the 1960s and 1970s during peak atmospheric $^{14}CO_2$ undergoes biogenic decay. Randerson et al. (2002) predict that during the early part of the 21st century several features of the latitudinal profile of $\Delta^{14}C$ will substantially change because of the partial release of bomb ^{14}C that has accumulated in the Southern Ocean, and continued fossil fuel emissions in the northern hemisphere.

Non-seasonal and inter-annual variability in $\Delta^{14}CO_2$

Inter-annual variability can be examined using the variation in seasonal cycle and amplitude, and the

variation in the residual component in the STL analysis of both $\Delta^{14}CO_2$ (Fig. 3c, d) and [$^{14}CO_2$] inventory (not shown).

Factors contributing to inter-annual variability include changes in both biospheric and oceanic fluxes due to climatic variability such as ENSO and the Southern Annular Mode (SAM), and variability in the cosmogenic production rate of ^{14}C.

An anomalously negative value for the Southern Oscillation Index (SOI, expressed as the atmospheric pressure difference between Darwin, Australia and Tahiti) is associated with El Nino conditions, and high positive values are indicative of La Nina conditions (Mullan 1996). During El Nino conditions the upwelling of deep, cold water in the western Pacific Ocean decreases, and the sea surface temperature in the eastern equatorial Pacific increases. During El Nino conditions enhanced uncontrolled biomass burning in the tropics is also more prevalent (Ropelewski and Halpert 1987). A 10-year periodicity in residual $\Delta^{14}CO_2$ was tentatively identified in the western Pacific Ocean which was potentially correlated with the ENSO signal (Kitagawa et al. 2004). In the early 1990s large seasonal variations in atmospheric $\Delta^{14}CO_2$ in the equatorial Pacific Ocean area were possibly due to ocean upwelling changes occurring during an El Nino event (Rozanski et al. 1995). There is no apparent correlation between SOI and $\Delta^{14}CO_2$ in either the seasonal component or the residual component in the Baring Head data record (Fig. 3).

Variations in cosmic ray intensity, related to changes in sunspot activity, result in variations of about 30% in the production rate of $^{14}CO_2$ in the stratosphere (Damon et al. 1973). Modeling studies predict an inverse relationship between the 11-year solar cycle and tropospheric radiocarbon concentration, with a 3‰ peak-to-trough amplitude and the $^{14}CO_2$ lagging by about 2 years (Damon et al. 1973). Atmospheric $^{14}CO_2$ concentrations, as recorded in tree-rings, are correlated with sunspot activity (Stuiver 1961; Tans et al. 1979), though this effect has been masked in recent years by the bomb signal. There is no apparent relationship between either the variability in seasonality or the residual components of the Wellington $\Delta^{14}CO_2$ signal with sunspot number.

The SAM has been identified as being a primary driver of interannual variability in the strength of the Southern Ocean CO_2 sink (Le Quere et al. 2007; Lenton and Matear 2007; Lovenduski and Gruber 2005) through the influence of the SAM on the intensity of the wind fields, and thus on ocean circulation and on CO_2 exchange fluxes. The effect of the SAM extends to the latitudes of New Zealand (Ummenhofer and England 2007) and strong variability in the air–sea CO_2 flux has been predicted to be related to SAM in the waters around New Zealand (Lenton and Matear 2007). The uptake of CO_2 in subantarctic water decreases during a positive SAM phase, with a time lag of 2 months. North of the subtropical front (located at 43–44°S in the South West Pacific Ocean) the response is in the opposite direction and the oceanic uptake is increased during a positive SAM phase. There is no apparent correlation between SAM (http://www.nerc-bas.ac.uk/icd/gjma/sam.html) and either the seasonal or residual component of the Wellington $\Delta^{14}CO_2$ record.

Conclusion

Tropospheric $\Delta^{14}CO_2$ data measured at Wellington, New Zealand for the period 1954–2005 are presented, and the local $^{14}CO_2$ mixing ratio (proportional to its broader tropospheric inventory) is derived using the $\Delta^{14}CO_2$ data, and the $^{14}CO_2$ mixing ratio. The $\Delta^{14}CO_2$ rose from a near-background level in 1954 to a peak in 1966 due to the input of bomb-derived $^{14}CO_2$, then fell as the ^{14}C-enriched CO_2 was transferred to the oceanic and biospheric reservoirs. In about 2000 the $^{14}CO_2$ mixing ratio plateaued and began to slowly increase consistently with forecasts of a nadir in the tropospheric $^{14}CO_2$ inventory (Caldeira et al. 1998) as a net efflux of tropospheric $^{14}CO_2$ gave way to a net influx. The relative importance and timing of the partitioning between the troposphere, stratosphere, biosphere, and ocean reservoirs are examined and interpreted using the GRACE model (Naegler and Levin 2006).

The $\Delta^{14}C$ time series are separated into long term, seasonal and residual components using a seasonal decomposition procedure (Cleveland 1979), and the seasonal and non-seasonal variability examined. The changing seasonal cycle is attributed to the decrease in the influence of outflow from the northern hemisphere stratosphere (where much of the bomb carbon was produced) and increases in the return

$^{14}CO_2$ fluxes from biosphere and Southern Ocean which have similar seasonal cycles.

The Wellington data are compared with $\Delta^{14}CO_2$ data available from 1987 (Levin et al. 2007) at Cape Grim in Tasmania, Australia, which has similar latitude. While the 19-year decline in excess $\Delta^{14}CO_2$ at both sites are comparable ($\sim$18 year e-folding time), the Wellington data showed several transitory features absent from the Cape Grim record that may be influences of the oceans surrounding New Zealand. The non-seasonal variations in the Wellington $\Delta^{14}CO_2$ data appear unrelated to climatic oscillations or to the solar cycle.

Acknowledgments The initial measurements undertaken by Rafter and Ferguson (1957) demonstrated the importance of this time series even in the first year. Maintaining a long term measurement programme such as the Wellington atmospheric $^{14}CO_2$ record requires the work of many people. We wish to acknowledge all those who have been involved in the data collection, site and equipment maintenance, extraction and measurement procedures and data analysis during the 51 years since the record began. Two Reviewers assisted greatly with their comments. The programme is jointly operated by NIWA and GNS Science, and is currently funded under NIWA contract C01X0204 to the New Zealand Foundation for Research, Science and Technology.

Appendix

$\Delta^{14}CO_2$ data from Wellington, New Zealand. Samples up to, and including, June 1987 were collected from Makara, those from July 1988 onwards were collected at Baring Head (see Fig. 1). Data from July 1985 until June 1987 that have been revised since being published by Manning et al. (1990) are indicated with a '#'. The dates given are the middle of the sample period. The $\delta^{13}C$ is of the CO_2 in the NaOH collection solution, not the atmosphere, and is used to correct for the fractionation of $^{14}CO_2$ during the collection process. The standard deviation (SD) associated with the $\Delta^{14}C$ value is calculated in one of two different ways, depending on the analysis method. For samples collected from 1954 to May 1995, the SD is the standard deviation associated with the proportional counting. The SD for samples collected from June 1995 and analysed by AMS is based on multiple measurements made on each sample (Table 3).

Table 3 $\Delta^{14}CO_2$ data from Wellington, New Zealand

Date	$\delta^{13}C$/‰	$\Delta^{14}C$/‰	SD in $\Delta^{14}C$/‰
15-Dec-1954	−9.4	−17.7	7.6
22-Feb-1955	−9.4	−10.1	7.7
14-Apr-1955	−9.4	−1.4	7.6
10-May-1955	−24.9	−10.3	7.8
15-Jun-1955	−9.4	−4.1	5.9
7-Sep-1955	−8.8	−11.9	4.0
15-Dec-1955	−8.8	0.1	5.4
19-Feb-1956	−8.8	5.6	3.9
15-Jun-1956	−25.0	37.9	4.8
25-Sep-1956	−25.8	10.1	4.8
21-Oct-1956	−9.0	13.6	4.7
22-Oct-1956	−9.2	18.1	4.7
27-Jan-1957	−9.0	18.3	3.7
27-Jan-1957	−10.1	24.9	3.7
28-Apr-1957	−10.6	39.0	4.7
28-Apr-1957	−9.8	41.5	4.7
22-May-1957	−24.8	16.6	4.8
23-Jul-1957	−9.4	44.9	3.9
23-Jul-1957	−9.6	43.4	3.9
27-Aug-1957	−24.8	51.4	4.0
9-Oct-1957	−12.5	46.3	5.1
6-Nov-1957	−9.7	51.6	4.7
26-Nov-1957	−8.8	62.0	4.6
18-Mar-1958	−9.4	67.5	4.0
18-Mar-1958	−10.1	76.2	4.0
4-Jul-1958	−25.0	81.1	3.8
28-Aug-1958	−25.0	77.8	3.8
29-Sep-1958	−24.8	93.9	3.5
9-Oct-1958	−24.6	116.9	4.6
23-Dec-1958	−25.0	110.1	3.8
17-Jan-1959	−25.0	121.1	3.8
2-Mar-1959	−25.0	126.0	4.6
11-Apr-1959	−25.1	137.2	3.8
1-Jun-1959	−25.9	132.8	3.8
13-Jul-1959	−25.2	150.1	3.8
13-Aug-1959	−25.0	141.8	4.5
1-Oct-1959	−26.4	164.6	4.5
19-Nov-1959	−24.5	171.4	4.5
19-Dec-1959	−25.0	181.7	4.5
21-Jan-1960	−25.2	181.8	4.5
14-Apr-1960	−23.4	187.9	4.5
14-Jul-1960	−24.0	187.4	4.5
1-Sep-1960	−22.8	193.7	4.5
29-Sep-1960	−22.5	195.9	4.5

Table 3 continued

Date	$\delta^{13}C$/‰	$\Delta^{14}C$/‰	SD in $\Delta^{14}C$/‰
13-Nov-1960	−26.4	198.4	4.5
19-Dec-1960	−24.5	193.7	4.5
20-Jan-1961	−25.5	194.9	4.5
10-Mar-1961	−24.9	207.1	5.1
14-Apr-1961	−25.0	201.9	4.5
26-May-1961	−26.3	196.7	4.5
6-Jul-1961	−25.1	198.3	9.5
19-Aug-1961	−25.3	197.9	6.3
3-Oct-1961	−24.7	182.8	5.0
11-Nov-1961	−23.8	237.2	9.4
19-Dec-1961	−25.1	227.3	9.4
19-Jan-1962	−24.6	197.4	5.0
2-Mar-1962	−23.4	207.3	7.5
25-Apr-1962	−24.5	214.3	5.1
25-May-1962	−24.5	189.4	9.5
28-Sep-1962	−24.5	233.5	4.4
9-Nov-1962	−24.0	250.4	5.9
20-Dec-1962	−28.4	266.6	3.9
18-Jan-1963	−25.9	265.5	3.9
1-Mar-1963	−23.6	269.7	3.9
1-Mar-1963	−23.6	266.4	3.8
14-Apr-1963	−23.5	280.9	3.8
14-Apr-1963	−23.5	284.3	3.9
26-May-1963	−24.2	313.2	4.1
6-Jul-1963	−24.7	331.1	4.1
17-Aug-1963	−24.7	355.6	4.3
29-Sep-1963	−23.7	405.2	3.8
10-Nov-1963	−24.7	374.8	4.1
20-Dec-1963	−24.7	429.5	3.8
17-Jan-1964	−23.1	445.7	3.8
1-Mar-1964	−22.8	472.5	4.0
11-Apr-1964	−23.7	500.3	4.0
23-May-1964	−25.9	498.3	3.9
3-Jul-1964	−24.7	542.4	3.7
15-Aug-1964	−24.6	567.4	4.0
3-Oct-1964	−25.4	507.0	3.9
6-Nov-1964	−24.7	621.9	3.9
17-Dec-1964	−19.9	615.7	3.9
15-Jan-1965	−22.0	689.4	7.5
27-Feb-1965	−23.6	633.6	3.9
8-Apr-1965	−23.9	634.1	3.9
21-May-1965	−21.4	615.2	3.8
2-Jul-1965	−25.7	694.5	3.9
13-Aug-1965	−23.9	614.1	3.9

Table 3 continued

Date	$\delta^{13}C$/‰	$\Delta^{14}C$/‰	SD in $\Delta^{14}C$/‰
24-Sep-1965	−25.2	634.2	4.0
6-Nov-1965	−18.1	625.7	4.0
24-Dec-1965	−24.9	634.4	3.9
4-Feb-1966	−24.6	647.3	3.9
8-Mar-1966	−26.4	646.5	3.9
2-Apr-1966	−23.9	631.8	3.6
20-May-1966	−26.1	622.1	3.8
10-Jun-1966	−25.0	612.4	4.2
6-Jul-1966	−23.2	612.2	4.4
19-Aug-1966	−24.8	590.8	3.9
9-Sep-1966	−26.8	625.2	3.8
7-Oct-1966	−23.8	614.8	3.9
5-Nov-1966	−25.1	614.9	4.2
11-Dec-1966	−24.8	627.8	3.9
9-Jan-1967	−24.6	616.4	3.9
24-Feb-1967	−23.0	602.9	4.4
8-Apr-1967	−23.4	609.0	3.8
6-May-1967	−23.7	596.5	3.8
10-Jun-1967	−23.7	580.0	6.3
10-Jun-1967	−23.7	595.9	5.4
19-Jul-1967	−24.4	571.3	3.8
6-Oct-1967	−23.1	575.1	3.8
10-Nov-1967	−25.7	586.0	5.2
9-Dec-1967	−24.4	579.6	3.9
13-Jan-1968	−23.9	583.0	3.9
11-Feb-1968	−24.5	582.5	3.9
11-Mar-1968	−22.5	572.8	3.6
6-Apr-1968	−23.9	547.6	3.7
31-May-1968	−24.8	560.5	3.9
7-Jun-1968	−24.6	561.7	3.9
5-Jul-1968	−26.3	550.4	3.9
9-Aug-1968	−24.7	538.1	3.9
30-Aug-1968	−23.8	535.5	3.8
6-Sep-1968	−23.7	531.5	3.9
4-Oct-1968	−24.6	532.8	3.9
18-Oct-1968	−24.7	537.6	3.9
2-Nov-1968	−25.3	541.9	3.9
8-Nov-1968	−26.9	541.2	3.9
6-Dec-1968	19–23.8	539.6	3.9
10-Jan-1969	−24.3	539.1	3.9
7-Feb-1969	−23.1	537.7	3.8
8-Mar-1969	−3.3	550.4	3.8
13-Apr-1969	−23.4	545.4	3.8
2-May-1969	−23.1	530.4	4.0

Table 3 continued

Date	$\delta^{13}C$/‰	$\Delta^{14}C$/‰	SD in $\Delta^{14}C$/‰
9-May-1969	−22.8	539.6	3.9
7-Jun-1969	−23.4	525.2	4.2
11-Jul-1969	−23.2	526.3	3.9
9-Aug-1969	−23.0	522.8	3.9
5-Sep-1969	−23.5	544.9	3.8
10-Oct-1969	−25.2	531.2	3.9
3-Nov-1969	−23.2	523.0	3.9
5-Dec-1969	−22.5	510.2	3.9
9-Jan-1970	−22.5	510.2	3.9
6-Mar-1970	−22.5	535.3	3.9
10-Apr-1970	−22.1	520.4	3.9
9-May-1970	−22.4	513.5	3.9
6-Jun-1970	−23.3	516.2	3.9
10-Jul-1970	−23.8	505.9	3.9
7-Aug-1970	−23.6	497.4	3.5
11-Sep-1970	−24.5	508.0	3.9
10-Oct-1970	−24.3	498.6	3.9
6-Nov-1970	−23.3	497.6	4.0
23-Dec-1970	−22.7	495.6	3.9
10-Jan-1971	−22.3	500.6	3.9
5-Feb-1971	−23.8	494.7	3.7
5-Mar-1971	−24.6	508.3	3.9
9-Apr-1971	−24.8	501.0	3.9
7-May-1971	−24.9	499.7	3.9
11-Jun-1971	−24.6	499.0	3.9
9-Jul-1971	−25.9	494.2	4.1
8-Aug-1971	−23.5	483.3	4.0
10-Sep-1971	−24.5	478.8	4.5
10-Oct-1971	−24.0	492.5	3.9
3-Dec-1971	−24.8	479.3	3.9
9-Jan-1972	−23.9	484.5	3.6
6-Feb-1972	−24.7	491.6	4.0
17-Mar-1972	−22.5	474.8	7.4
31-Mar-1972	−23.8	482.4	3.6
20-Apr-1972	−22.6	468.1	3.6
4-May-1972	−23.0	469.5	5.1
10-Jun-1972	−24.4	470.1	5.1
7-Jul-1972	−24.0	465.9	5.1
1-Sep-1972	−24.7	450.3	5.1
7-Oct-1972	−24.4	449.9	6.7
8-Dec-1972	−24.9	447.3	4.7
10-Feb-1973	−24.3	453.9	5.1
9-Mar-1973	−23.6	442.8	3.3
6-Jul-1973	−24.7	435.0	3.7

Table 3 continued

Date	$\delta^{13}C$/‰	$\Delta^{14}C$/‰	SD in $\Delta^{14}C$/‰
11-Aug-1973	−24.5	427.1	3.3
7-Sep-1973	−24.4	415.9	3.7
6-Oct-1973	−24.1	426.0	3.3
9-Nov-1973	−23.4	434.3	3.7
7-Dec-1973	−23.3	417.2	3.2
11-Jan-1974	−23.2	412.8	3.5
1-Feb-1974	−23.0	405.1	3.3
8-Mar-1974	−22.2	418.5	3.3
4-Apr-1974	−23.0	417.2	3.3
10-May-1974	−23.3	386.8	3.3
7-Jun-1974	−23.3	359.7	3.3
6-Jul-1974	−23.3	394.5	3.3
7-Aug-1974	−24.8	392.3	3.7
6-Sep-1974	−23.4	405.0	3.3
5-Oct-1974	−23.2	398.7	4.7
8-Nov-1974	−22.8	401.7	3.3
8-Dec-1974	−23.4	393.7	3.3
10-Jan-1975	−22.2	396.3	3.3
7-Feb-1975	−23.4	399.0	3.7
7-Mar-1975	−23.3	400.6	3.3
5-Apr-1975	−23.4	397.7	3.3
10-May-1975	−23.2	389.1	3.7
20-Jun-1975	−23.9	384.5	3.3
9-Jul-1975	−23.1	377.3	3.3
10-Aug-1975	−24.9	378.1	3.7
12-Sep-1975	−26.2	367.5	3.7
3-Oct-1975	−23.6	354.0	8.8
10-Oct-1975	−22.4	365.3	3.3
15-Nov-1975	−23.0	363.8	3.7
5-Dec-1975	−23.6	370.8	3.7
13-Jan-1976	−23.8	373.4	3.7
6-Feb-1976	−24.3	368.1	3.3
6-Mar-1976	−23.7	366.7	3.1
10-Apr-1976	−23.0	346.1	3.3
10-May-1976	−22.9	359.6	3.3
6-Jun-1976	−25.0	360.9	3.4
4-Jul-1976	−22.2	365.0	5.0
15-Aug-1976	−23.9	343.3	3.7
11-Oct-1976	−22.9	344.2	5.1
4-Nov-1976	−25.3	346.5	3.3
10-Dec-1976	−23.6	329.6	3.7
3-Jan-1977	−24.5	332.9	3.7
11-Feb-1977	−24.3	347.0	5.3
11-Mar-1977	−24.7	335.4	4.5

Table 3 continued

Date	$\delta^{13}C$/‰	$\Delta^{14}C$/‰	SD in $\Delta^{14}C$/‰
6-May-1977	−24.8	332.9	3.3
12-Jun-1977	−24.1	335.6	4.7
15-Jul-1977	−22.4	331.5	3.7
13-Aug-1977	−24.1	323.6	3.3
9-Sep-1977	−24.8	317.6	3.3
1-Oct-1977	−28.1	335.1	3.4
7-Oct-1977	−24.2	322.0	3.7
11-Nov-1977	−23.4	325.0	3.7
2-May-1978	−24.6	314.6	3.7
11-Jun-1978	−25.8	310.4	3.7
30-Jun-1978	−25.9	314.8	3.7
4-Aug-1978	−25.2	308.8	3.2
8-Sep-1978	−18.0	309.0	5.1
7-Oct-1978	−25.5	321.3	8.9
10-Nov-1978	−25.4	308.1	3.3
12-Jan-1979	−24.9	310.2	3.3
17-Mar-1979	−24.7	302.8	3.3
7-Apr-1979	−25.3	304.2	3.7
9-May-1979	−24.9	296.2	3.2
3-Jun-1979	−24.5	292.3	3.3
10-Jul-1979	−24.9	298.6	3.8
12-Aug-1979	−25.4	284.0	3.8
5-Oct-1979	−25.3	282.9	3.7
3-Nov-1979	−25.2	303.5	3.8
9-Dec-1979	−24.3	276.4	3.3
12-Feb-1980	−25.3	282.3	3.3
8-Mar-1980	−25.1	289.0	3.8
4-Apr-1980	−24.8	277.6	3.3
8-May-1980	−23.7	279.4	3.3
6-Jul-1980	−25.4	281.5	3.7
1-Aug-1980	−25.0	274.3	3.7
5-Sep-1980	−24.8	278.1	3.3
9-Oct-1980	−25.5	282.7	3.7
11-Nov-1980	−25.6	272.9	3.2
4-Dec-1980	−25.4	268.6	3.4
10-Jan-1981	−24.7	266.0	3.7
6-Feb-1981	−25.4	260.9	3.7
12-Mar-1981	−24.0	264.1	4.7
10-Apr-1981	−25.2	270.9	3.3
6-Jun-1981	−26.2	263.3	3.7
9-Aug-1981	−26.1	259.5	3.3
4-Sep-1981	−25.1	258.0	5.1
2-Oct-1981	−26.0	256.8	3.3
1-Nov-1981	−25.4	254.7	3.7

Table 3 continued

Date	$\delta^{13}C$/‰	$\Delta^{14}C$/‰	SD in $\Delta^{14}C$/‰
3-Dec-1981	−25.4	254.8	3.2
9-May-1982	−23.5	245.2	3.2
5-Jun-1982	−25.0	248.5	3.2
8-Jul-1982	−23.3	249.2	3.8
2-Sep-1982	−25.8	241.3	3.2
6-Dec-1982	−25.2	235.5	3.4
17-Jan-1983	−24.1	233.6	3.7
7-Feb-1983	−24.9	227.4	3.7
6-Mar-1983	−25.8	233.9	3.3
7-Jun-1983	−25.2	235.6	3.7
19-Aug-1983	−25.0	235.0	3.7
15-Oct-1983	−24.9	221.2	3.7
15-Jan-1984	−25.0	217.5	3.3
5-Feb-1984	−24.2	230.3	3.8
8-May-1984	−25.3	214.0	3.8
9-Jul-1984	−25.3	214.5	3.8
3-Aug-1984	−26.4	238.0	4.4
10-Sep-1984	−25.4	208.1	3.5
11-Nov-1984	−25.4	206.9	2.7
2-Dec-1984	−26.4	216.8	3.3
2-Feb-1985	−26.5	206.9	3.3
24-Mar-1985	−25.4	209.8	3.8
5-Jul-1985[#]	−27.2	216.2[#]	9.4[#]
8-Aug-1985[#]	−25.7	212.6[#]	6.4[#]
9-Sep-1985	−25.8	202.9[#]	6.4[#]
1-Nov-1985[#]	−26.0	203.8[#]	4.8[#]
2-Dec-1985	−26.6	205.4[#]	4.8[#]
20-Jan-1986[#]	−23.7	204.6[#]	3.8[#]
18-Feb-1986[#]	−26.0	203.4[#]	6.4[#]
30-Mar-1986[#]	−25.9[#]	199.6[#]	5.5[#]
4-Apr-1986[#]	−25.6	189.2[#]	6.3[#]
3-May-1986[#]	−23.5[#]	183.6[#]	7.2[#]
12-Jul-1986	−25.8	194.7[#]	4.9[#]
9-Aug-1986[#]	−26.5	188.5[#]	4.1[#]
6-Sep-1986[#]	−26.1	200.7[#]	4.1[#]
4-Oct-1986[#]	−26.0	194.0	4.8[#]
7-Nov-1986[#]	−25.5	191.0	4.8[#]
7-Dec-1986	−25.6	189.4[#]	4.8[#]
3-Jan-1987	−25.5	186.7[#]	4.8[#]
10-May-1987	−25.5	185.8[#]	4.8[#]
11-Jun-1987[#]	−25.8	176.3[#]	5.4[#]
15-Jul-1988	−25.4	175.7	6.4
15-Aug-1988	−25.6	176.1	6.7
19-Sep-1988	−26.5	167.3	5.9

Table 3 continued

Date	$\delta^{13}C$/‰	$\Delta^{14}C$/‰	SD in $\Delta^{14}C$/‰
23-Oct-1988	−26.3	178.4	7.9
25-Nov-1988	−24.9	178.6	3.2
16-Dec-1988	−24.6	169.2	3.5
28-Jan-1989	−23.5	175.4	3.6
19-Feb-1989	−24.7	167.2	3.8
21-May-1989	−25.0	162.8	3.5
24-Jun-1989	−24.8	164.5	3.5
3-Aug-1989	−22.5	164.6	3.8
26-Aug-1989	−24.2	160.5	3.8
12-Dec-1989	−24.8	161.0	3.8
20-Jan-1990	−24.5	154.0	3.9
18-Feb-1990	−23.7	173.7	3.5
22-Apr-1990	−27.5	164.1	3.8
12-Jul-1990	−23.4	160.4	3.9
16-Aug-1990	−25.4	159.0	4.7
17-Sep-1990	−24.6	162.3	3.3
9-Nov-1990	−26.7	162.9	4.8
14-Dec-1990	−24.2	162.9	3.5
15-Jan-1991	−23.8	154.1	3.8
17-Feb-1991	−23.0	157.2	4.1
18-Mar-1991	−25.7	169.0	3.6
29-Apr-1991	−26.0	164.9	11.9
22-May-1991	−24.9	163.0	6.7
20-Jun-1991	−22.2	164.2	3.4
19-Jul-1991	−22.8	162.6	5.7
1-Sep-1991	−21.0	158.5	3.3
19-Sep-1991	−22.7	155.3	3.5
17-Oct-1991	−23.4	162.6	2.9
6-Dec-1991	−24.4	149.8	3.6
27-Jan-1992	−24.2	155.9	4.5
22-Feb-1992	−24.0	156.5	3.2
5-Apr-1992	−22.9	161.4	2.7
30-Apr-1992	−21.2	165.6	3.2
29-Jul-1992	−24.5	160.9	6.0
23-Aug-1992	−25.6	139.0	4.5
8-Oct-1992	−21.2	149.2	4.8
28-Oct-1992	−18.9	143.3	3.2
6-Jan-1993	−18.1	146.7	3.8
23-Feb-1993	−21.1	140.3	2.9
31-Mar-1993	−20.5	132.6	3.5
9-May-1993	−25.1	135.0	3.7
10-Jul-1993	−22.4	125.6	3.1
2-Aug-1993	−21.2	129.2	3.2
18-Sep-1993	−23.7	133.6	3.5

Table 3 continued

Date	$\delta^{13}C$/‰	$\Delta^{14}C$/‰	SD in $\Delta^{14}C$/‰
18-Feb-1994	−20.7	132.6	4.9
3-Apr-1994	−24.1	127.1	3.9
7-Jun-1994	−22.8	131.5	3.7
15-Jul-1994	−24.2	125.7	3.9
30-Aug-1994	−24.4	121.4	3.6
27-Oct-1994	−15.6	128.4	6.3
23-Nov-1994	−25.7	124.7	3.9
25-Dec-1994	−23.7	128.4	3.6
25-Jan-1995	−24.1	127.4	3.4
4-Mar-1995	−24.4	115.7	3.5
7-Apr-1995	−21.5	118.1	3.6
9-May-1995	−22.1	113.7	3.5
20-Jun-1995	−23.5	106.9	4.1
13-Jul-1995	−25.1	111.2	4.3
31-Aug-1995	−23.3	113.3	4.0
16-Sep-1995	−24.4	117.6	4.3
2-Oct-1995	−22.7	116.4	4.1
29-Nov-1995	−19.3	108.1	5.4
27-Dec-1995	−21.0	106.7	4.9
13-Jan-1996	−22.0	110.4	4.2
31-Jan-1996	−22.0	115.2	4.1
26-Feb-1996	−16.4	111.3	4
8-Apr-1996	−23.0	113.8	4.4
20-Sep-1996	−21.3	116.1	3.6
18-Oct-1996	−21.6	118.6	4.1
30-Jan-1997	−23.5	111.9	3.9
10-Mar-1997	−18.8	105.6	3.9
14-May-1997	−15.5	109.0	4
7-Jul-1999	−24.5	102.3	
17-Jul-1999	−21.1	95.6	3.7
11-Aug-1999	−22.8	78.2	4
1-Oct-1999	−20.6	89.6	4
21-Oct-1999	−17.6	94.1	6.6
8-Dec-1999	−12.6	107.6	1.2
20-Jan-2000	−16.7	87.3	3.4
29-Jan-2000	−22.1	72.7	4.9
5-Feb-2000	−16.9	86.5	5
26-Mar-2000	−21.1	81.2	7.9
18-Apr-2000	−16.8	84.8	3.2
10-May-2000	−18.5	80.4	3.2
31-May-2000	−22.5	81.8	3.2
20-Jun-2000	−22.0	75.7	3.3
18-Sep-2000	−24.4	95.1	3.7
29-Sep-2000	−22.5	94.7	3.5

Table 3 continued

Date	$\delta^{13}C$/‰	$\Delta^{14}C$/‰	SD in $\Delta^{14}C$/‰
14-Oct-2000	−25.5	91.0	3.2
19-Nov-2000	−12.0	96.6	3.3
12-Jan-2001	−22.3	92.4	3.1
11-Mar-2001	−24.8	86.1	4.4
25-Mar-2001	−22.3	92.9	3.6
25-Sep-2001	−19.7	77.5	2.6
10-Oct-2001	−20.2	77.4	2.9
24-Oct-2001	−19.6	80.7	2.8
7-Nov-2001	−20.7	75.7	3.6
3-Dec-2001	−19.1	85.0	3.7
15-Dec-2001	−17.0	83.8	3.2
29-Dec-2001	−17.6	80.6	2.8
10-Jan-2002	−15.0	77.2	2.4
8-Mar-2002	−12.7	79.0	2.7
1-Apr-2002	−21.3	89.7	2.9
1-May-2002	−20.0	88.1	2.3
16-May-2002	−19.0	82.0	3.2
30-May-2002	−19.3	86.6	2.6
15-Jun-2002	−19.8	77.5	2.5
5-Jul-2002	−19.0	84.6	3.5
19-Jul-2002	−19.0	78.1	2.4
31-Jul-2002	−19.0	87.3	2.3
14-Aug-2002	−19.4	83.0	2.4
4-Sep-2002	−24.2	88.6	2.7
21-Sep-2002	−19.1	79.0	2.6
9-Oct-2002	−19.9	86.4	2.5
31-Oct-2002	−16.8	73.5	3.5
29-Nov-2002	−18.4	85.8	2.7
26-Dec-2002	−17.1	82.6	3.3
15-Jan-2003	−18.8	86.0	2.6
1-Feb-2003	−18.7	81.3	2.6
4-Mar-2003	−14.2	81.9	2.4
3-Apr-2003	−18.0	81.2	2.7
19-Apr-2003	−17.6	89.5	4.2
10-May-2003	−19.1	87.0	3.7
1-Jun-2003	−18.3	82.2	2.5
21-Jun-2003	−19.3	94.4	4.8
8-Jul-2003	−19.6	83.1	3.8
21-Jul-2003	−18.5	80.0	1.9
5-Sep-2003	−19.4	77.2	1.9
8-Oct-2003	−18.9	80.1	2.4
19-Nov-2003	−18.0	79.0	2
27-Dec-2003	−19.4	81.8	4.3
1-Feb-2004	−17.5	70.1	2.1
6-Mar-2004	−18.5	72.9	2.1
9-Apr-2004	−19.2	66.8	2.1
25-May-2004	−18.2	71.2	1.8
24-Jun-2004	−20.8	71.7	2.2
19-Aug-2004	−10.8	82.0	4.8
9-Nov-2004	−19.4	73.9	2.3
26-Nov-2004	−19.1	69.6	1.85
13-Dec-2004	−18.6	71.2	2.75
31-Dec-2004	−18.1	65.5	1.86
19-Jan-2005	−19.2	73.3	3.39
10-Feb-2005	−16.6	68.9	1.93
8-Mar-2005	−17.0	63.8	4.66
29-Mar-2005	−19.9	71.4	2.3
29-Mar-2005	−18.0	74.5	2.3
16-Apr-2005	−18.4	80.5	2.1
16-Apr-2005	−19.1	77.4	2.0
4-May-2005	−19.2	72.3	1.91
18-May-2005	−18.4	70.4	1.94

References

Allison CE, Francey RJ (2007) Verifying southern hemisphere trends in atmospheric carbon dioxide stable isotopes. J Geophys Res 112(D21304). doi:10.1029/2006JD007345

Appenzeller C, Holton JR, Rosenlof KH (1996) Seasonal variation of mass transport across the tropopause J. Geophys. Res. 101(D10):15071–15078

Broecker WS, Peng T-H, Takahashi T (1980) A strategy for the use of bomb-produced radiocarbon as a tracer for the transport of fossil fuel CO_2 into the deep-sea source regions. Earth Planet Sci Lett 49:463–468

Broecker WS, Peng T-H, Ostlund G, Minze S (1985) The distribution of bomb radiocarbon in the ocean. J Geophys Res 90(C4):6953–6970

Cain WF, Suess HE (1976) Carbon 14 in tree rings. J Geophys Res 81(21):3688–3694

Caldeira K, Rau GH, Duffy PB (1998) Predicted net efflux of radiocarbon from the ocean and increase in atmospheric radiocarbon content. Geophys Res Lett 25(20):3811–3814

Cleveland WS (1979) Robust locally weighted regression and smoothing scatterplots. J Am Stat Assoc 74:829–836

Cleveland WS, Freeny AE, Graedel TE (1983) The seasonal component of atmospheric CO_2: information from new approaches to the decomposition of seasonal time series. J Geophys Res 88(C15):10934–10946

Damon PE, Long A, Wallick EI (1973) On the magnitude of the 11-year radiocarbon cycle. Earth Planet Sci Lett 20:300–306

Donahue DJ, Linick TW, Jull AJT (1990) Isotope-ratio and background correction for accelerator mass spectrometry radiocarbon measurements. Radiocarbon 32(2):135–142

Druffel EM, Suess HE (1983) On the radiocarbon record in banded corals: exchange parameters and net transport of $^{14}CO_2$ between atmosphere and surface ocean. J Geophys Res 88:1271–1280

Francey RJ, Allison CE, Etheridge DM, Trudinger CM, Enting IG, Leuenberger M, Langenfelds RL, Michel E, Steele LP (1999) A 1000-year high precision record of $\delta^{13}C$ in atmospheric CO_2. Tellus 51B:170–193

Gomez AJ (1996) Baring head atmospheric data summary. NIWA Science and Technology series 39

Hartley DE, Black RX (1995) Mechanistic analysis of interhemispheric transport. Geophys Res Lett 22(21): 2945–2948

Hesshaimer V, Heimann M, Levin I (1994) Radiocarbon evidence for a smaller oceanic carbon dioxide sink than previously believed. Nature 370:201–203

Hua Q, Barbetti M (2004) Review of tropospheric bomb ^{14}C data for carbon cycle modeling and age calibration purposes. Radiocarbon 46(3):1273–1298

Karlen I, Olsen IU, Kallberg P, Kilicci S (1964) Absolute determination of the activity of two 14C dating standards. Arkiv For Geofysik Band 4(22):465–471

Keeling CD, Whorf TP (2005) Atmospheric CO_2 records from sites in the SIO air sampling network. In: Trends: a compendium of data on global change. Carbon Dioxide Information Analysis Center, Oak Ridge National Laboratory

Kitagawa H, Mukai H, Nojiri Y, Shibata Y, Kobayashi T, Nojiri T (2004) Seasonal, secular variation of atmospheric 14CO2 over the Western Pacific since 1994. Radiocarbon 46(2):901–910

Le Quere C, Rodenbeck C, Buitenhuis ET, Conway TJ, Langenfelds R, Gomez A, Labuschagne C, Ramonet M, Nakazawa T, Metzl N, Gillett N, Heimann M (2007) Saturation of the Southern Ocean CO_2 sink due to recent climate change. Science 316:1735–1738. doi:1710.1126/science.116188

Lenton A, Matear RJ (2007) Role of the Southern Annular mode (SAM) in Southern Ocean CO_2 uptake. Global Biogeochem. Cycles 21. doi:10.1029/2006GB02714

Levchenko VA, Etheridge DM, Francey RJ, Trudinger C, Tuniz C, Lawson EM, Smith AM, Jacobsen GE, Hua Q, Hotchkis MAC, Fink D, Morgan V, Head J (1997) Measurements of the $^{14}CO_2$ bomb pulse in firn and ice at Law Dome, Antarctica. Nucl Instrum Methods Phys Res B 123:290–295

Levin I, Hesshaimer V (2000) Radiocarbon—a unique tracer of global carbon cycle dynamics. Radiocarbon 42(1): 69–80

Levin I, Munnich KO, Weiss W (1980) The effect of anthropogenic CO_2 and ^{14}C sources on the distribution of ^{14}C in the atmosphere. Radiocarbon 22(2):379–391

Levin I, Kromer B, Shoch-Fischer H, Bruns M, Munnich M, Berdau D, Vogel JC, Munnich KO (1985) 25 years of tropospheric 14C observations in Central Europe. Radiocarbon 27(1):1–19

Levin I, Graul R, Trivett NBA (1995) Long term observations of atmospheric CO_2 and carbon isotopes at continental sites in Germany. Tellus 47B:23–34

Levin I, Kromer B, Steele LP, Porter LW (2007) Continuous measurements of 14C in atmospheric CO2 at Cape Grim, 1997–2006. In: Cainey JM, Derek N, Krummel PB (eds) Baseline Atmospheric Program Australia 2005–2006. Australian Bureau of Meteorology and CSIRO Marine and Atmospheric Research, Melbourne, pp 57–59

Lovenduski NS, Gruber N (2005) Impact of the Southern Annular mode on Southern Ocean circulation and biology. Geophys Res Lett 32(L11603). doi:10.1029/2005GL022727

Manning MR, Melhuish WH (1994) $\Delta^{14}CO_2$ record from Wellington. In: Boden TA, Kaiser DP, Sepanski FJ, Stoss FW (eds) Trends 93—a compendium of data on global change. DCIAC, Oak Ridge, pp 173–202

Manning MR, Lowe DC, Melhuish WH, Sparks RJ, Wallace G, Breninkmeijer CAM, McGill RC (1990) The use of radiocarbon measurements in atmospheric studies. Radiocarbon 32:37–58

Meijer HAJ, van der Plicht J, Gislefoss JS, Nydal R (1995) Comparing long-term atmospheric ^{14}C and ^{3}H records near Groningen, Netherlands with Fruholmen, Noway and Izana, Canary Islands. Radiocarbon 37(1):39–50

Milton GM, Kramer SJ (1998) Using 14C as a tracer of carbon accumulation and turnover in soils. Radiocarbon 40:999–1011

Mullan AB (1996) Non-linear effects of the Southern Oscillation in the New Zealand region. Aust Meteorl Mag 45:83–99

Naegler T, Levin I (2006) Closing the global radiocarbon budget 1945–2005. J Geophys Res 111(D12311). doi:10.1029/2005JD006758

Nydal R, Gislefoss JS (1996) Further application of bomb ^{14}C as a tracer in the atmosphere and ocean. Radiocarbon 38(3):389–406

Nydal R, Lovseth K (1983) Tracing bomb 14C in the atmosphere 1962–1980. J Geophys Res 88(C6):3621–3642

O'Brien BJ (1986) The use of natural and anthropogenic ^{14}C to investigate the dynamics of soil organic carbon. Radiocarbon 28:358–362

Rafter TA (1955) ^{14}C variations in nature and the effect on radiocarbon dating. N Z J Sci Technol 37(1):20–38

Rafter TA, Fergusson GJ (1957) The atom bomb effect: recent increase in the ^{14}C content of the atmosphere, biosphere, and surface waters of the oceans. N Z J Sci Technol 38(8):871–883

Rafter TA, Fergusson GJ (1959) Atmospheric radiocarbon as a tracer in geophysical circulation problems. In: United Nations peaceful uses of atomic energy. Pergamon Press, London

Randerson JT, Enting IG, Schuur EAG, Caldeira K, Fung IY (2002) Seasonal and latitudinal variability of troposphere $\Delta^{14}CO_2$: post bomb contributions from fossil fuels, oceans, the stratosphere, and the terrestrial biosphere. Global Biogeochem Cycles 16(4):1112. doi:1110.1029/2002GB001876

Ropelewski CF, Halpert MS (1987) Global and regional scale precipitation patterns associated with the El Nino/Southern oscillation. Mon Weather Rev 115:1606–1626

Rozanski K, Levin I, Stock J, Falcon REG, Rubio F (1995) Atmospheric $^{14}CO_2$ variation in the equatorial region. Radiocarbon 37(2):509–515

Stuiver M (1961) Variations in radiocarbon concentration and sunspot activity. J Geophys Res 66(1):273–276

Stuiver M, Polach HA (1977) Reporting of 14C data. Radiocarbon 19(3):355–363

Stuiver M, Quay PD (1981) Atmospheric ^{14}C changes resulting from fossil fuel CO_2 release and cosmic ray flux variability. Earth Planet Sci Lett 53:349–362

Suess HE (1955) Radiocarbon concentration in the modern world. Science 122:415–417

Tans PP, de Jong AFM, Mook WG (1979) Natural atmospheric ^{14}C variation and the Suess effect. Nature 280:826–828

Ummenhofer CC, England MH (2007) Interannual extremes in New Zealand precipitation linked to modes of Southern Hemisphere climate variability. J Clim 20(21):5418–5440